Small Cell Traffic Balancing Over Licensed and Unlicensed Bands

Feilu Liu, Erdem Bala, Elza Erkip, Mihaela C. Beluri and Rui Yang

arXiv:1501.00203v1 [cs.NI] 31 Dec 2014

Abstract—**The 3rd Generation Partnership Project (3GPP) recently started standardizing the "Licensed-Assisted Access using LTE" for small cells, referred to as Dual Band Femtocell (DBF) in this paper, which uses LTE air interface in both licensed and unlicensed bands based on the Long Term Evolution (LTE) carrier aggregation feature. Alternatively, the Small Cell Forum introduced the Integrated Femto-WiFi (IFW) small cell which simultaneously accesses both the licensed band (via cellular interface) and the unlicensed band (via WiFi interface). In this paper, a practical algorithm for IFW and DBF to automatically balance their traffic in licensed and unlicensed bands, based on the real-time channel, interference and traffic conditions of both bands is described. The algorithm considers the fact that some "smart" devices (sDevices) have both cellular and WiFi radios while some WiFi-only devices (wDevices) may only have WiFi radio. In addition, the algorithm considers a realistic scenario where a single small cell user may simultaneously use multiple sDevices and wDevices via either the IFW, or the DBF in conjunction with a Wireless Local Area Network (WLAN). The goal is to maximize the total user satisfaction/utility of the small cell user, while keeping the interference from small cell to macrocell below predefined thresholds. The algorithm can be implemented at the Radio Link Control (RLC) or the network layer of the IFW and DBF small cell base stations. Results demonstrate that the proposed traffic-balancing algorithm applied to either IFW or DBF significantly increases sum utility of all macrocell and small cell users, compared with the current practices. Finally, various implementation issues of IFW and DBF are addressed.**

Index Terms—**LTE-Unlicensed, LTE-U, Licensed-Assisted Access using LTE, traffic balancing, femtocell, 802.11, unlicensed band.**

I. INTRODUCTION

Small cells as part of the second tier in multi-tiered cellular networks have been considered as an effective means to boost the capacity and expand the coverage. Two types of small cells are widely used. One is the femtocell which shares the cellular

licensed band with macrocells [1], [2]. The other type is the WiFi hotspot that is built by cellular operators to offload traffic from their licensed bands to the unlicensed band. Fig. 1 shows the spectrum map of these two approaches in Cases 1 and 2, respectively.

In this paper, we use the terminology "device" to refer to the end-user terminal in Long Term Evolution (LTE) and WiFi communications, which is referred to as the user equipment (UE) in 3rd Generation Partnership Project (3GPP) terminology and the "station" in IEEE 802.11 WiFi terminology. Today many "smart" devices such as smartphones, tablets and iPads are equipped with both WiFi and cellular interfaces. In order to improve the data rate of such smart devices (sDevices), the Small Cell Forum proposed the Integrated Femto-WiFi (IFW) [3] which can simultaneously communicate in both the licensed band (via cellular interface) and the unlicensed band (via WiFi interface) with sDevices. The IFW spectrum usage is shown in Case 3 of Fig. 1.

An alternative way of simultaneously using both the licensed and unlicensed bands is investigated in our earlier study [4] which proposes that femto cells can use LTE technology in both licensed and unlicensed bands through the LTE carrier aggregation feature [5], resulting in the Dual-Band Femtocell (DBF) in Case 4 of Fig. 1. In September 2014, the 3GPP approved the industry proposal [6] to start standardizing the "Licensed-Assisted Access using LTE" which is also often referred to as LTE-Unlicensed, LTE-U and U-LTE. The main idea of LTE-U is the same as the DBF framework in this paper. Since the unlicensed spectrum is shared by many cellular operators and non-cellular devices, how to access the unlicensed band and how to share the unlicensed band with other devices is essential to the DBF user experience. However, these issues have not been addressed in [6] and may be an important part of the standardization effort.

Short-range data communications arising in small cells typically contain different types of devices. One type is the sDevice which is equipped with both WiFi and cellular interfaces as discussed above. We consider LTE as the cellular Radio Access Technology (RAT) in this paper in order to use the LTE carrier aggregation feature for DBF. Another type is the WiFi-only device (wDevice) such as TV, desktop computer, wireless printer and video surveillance camera, which is typically equipped with WiFi but no cellular interface. Cellular-only devices are not considered, as the most recent cellular devices typically have a WiFi interface. In addition, a single user may use multiple devices at the same time. For example, in a residential scenario, a user may be watching video clips on her tablet jointly over the WiFi and cellular

	Case 1: Cellular WiFi Hotspot		Case 2: Femto cell		Case 3: Integrated Femto-WiFi		Case 4: Dual-Band Femto	
	Lic	*Unlic*	*Lic*	*Unlic*	*Lic*	*Unlic*	*Lic*	*Unlic*
Cellular Small Cell		**WiFi**	**LTE**		**LTE**	**WiFi**	**LTE**	**LTE**

Fig. 1. Spectrum and radio access technologies used by each type of small cell. Long Term Evolution (LTE) and WiFi represent the air interfaces used in a band; blank box means the spectrum is not used.

interfaces (using IFW or DBF), while her wireless video surveillance camera continuously transfers live video to the WiFi access point (AP). Therefore, a user's satisfaction can come from the overall experience from multiple sDevices and wDevices. In Cases 1 and 3, the small cell (WiFi hotspot and IFW) can serve both sDevices and wDevices. However, in Cases 2 and 4, the cellular small cell itself (femto cell and DBF respectively) cannot serve wDevices, hence we assume the femto cell and DBF are deployed with non-cellular wireless local area network (WLAN) APs which are not physically integrated with the femto or DBF base station (BS) in the same box. The four use cases are summarized in Fig. 2. In the figure and throughout this paper, we denote macro BS and device by mBS and mDevice, respectively, and small cell (of Cases 1, 2, 3 and 4) BS as fBS.

In this study, the "small cell" mainly refers to the cell for short-range communications in residential and enterprise scenarios, as shown in the four use cases in Fig. 2; "macro cell" refers to pico, micro or macro cells. In addition, the "WiFi" refers to the air interface defined by the IEEE 802.11 standards; the "WiFi hotspot" only refers to the cellular small cell in Case 1; the "WLAN" only refers to the non-cellular networks used by the wDevices in Case 2 and 4.

The focus of this paper is on the Cases 3 and 4 which is defined in Fig. 2 and illustrated in Fig. 3. The contribution can be summarized as follows.

- In order for DBF to use the LTE air interface in the un-licensed band, we propose a channel access scheme that aligns with the LTE frame structure. Once the channel is obtained, the DBF will follow the standard LTE air interface in the unlicensed band.
- We propose a dynamic traffic balancing algorithm over licensed and unlicensed bands for IFW and DBF that aims at optimizing the overall *user experience* from multiple sDevices and wDevices in short range communications. The algorithm is based on the real-time channel, interference and traffic conditions of both bands. We formulate and solve for the optimal downlink traffic balancing scheme in order to maximize the user utility (satisfaction) from all sDevices and wDevices belonging to the same user while controlling the interference leaked from the small cell to the macrocell.
- The utility maximization described in the previous bullet is achieved by small cell power control in the licensed band and channel time allocation in the unlicensed band. Once the optimal channel time usage in the unlicensed band is determined, the small cell tunes its channel access parameters to achieve the allocated channel time. The process of tuning channel access parameters depends on

the RAT used in the unlicensed band. We study how the channel access parameters can be tuned for the IFW, which uses the WiFi air interface, and for the DBF, which uses the LTE air interface in the unlicensed band, respectively.
- We provide extensive system simulations that show that the proposed traffic balancing algorithm significantly improves user satisfaction for IFW and DBF, compared with the current practice where devices typically have to choose only one band (licensed or unlicensed) to use at a time, as in Cases 1 and 2 of Fig. 1.

This paper extends our earlier DBF traffic balancing algorithm [7] by considering multiple non-cellular WLAN devices, incorporating the IFW scenario, and introducing a new use case where a single user may use multiple devices. Both this paper and [7] are based on the channel access scheme proposed in our earlier study [4]. This work is related to [8] which proposes that LTE small cells use the licensed-exempt TV whitespace band. It is proposed in [8] that LTE small cells use frequency-hopping and time-hopping in the TV whitespace band to reduce interference from other devices in the band; whereas this study proposes a channel-sensing based channel access scheme for LTE small cells to access the band and reduce interference, which may also be applicable to the new Study Item (SI) "Licensed-Assisted Access using LTE" which was recently approved for 3GPP Rel-13 [6]. In addition, the existing literature on unlicensed band LTE [8] [9] does not investigate the traffic balancing problem over the two bands.

Existing traffic balancing algorithms over licensed and un-licensed bands are mainly for IFW [10] [11], but not for DBF. Specifically, Bennis et. al. [10] propose a cross-system learning framework by considering the QoS in traffic balancing and assuming no WiFi-only devices. Elsherif et. al [11] consider both "smart" and WiFi-only devices in traffic balancing, with the goal of maximizing the total throughput, but it does not tackle the problem from the perspective of user experience.

The paper is organized as follows. In Sec. II, we provide the system model. In Sec. III, we introduce a centralized channel access scheme for DBF to use the unlicensed band. In Sec. IV, we propose a traffic balancing algorithm for small cells to assign traffic over the licensed and unlicensed bands. The RAT-dependent process of tuning channel access parameters is analyzed in Sec. V for IFW and in Sec. VI for DBF. In Sec. VII, we evaluate the proposed traffic balancing algorithm through system simulations. In Sec. VIII, we conclude the paper and compare IFW and DBF from an implementation standpoint.

User and device	Network	Case 1: Cellular WiFi Hotspot		Case 2: Separate Femto + WLAN		Case 3: Integrated Femto-WiFi		Case 4: Dual-Band Femto + WLAN	
		Lic	Unlic	Lic	Unlic	Lic	Unlic	Lic	Unlic
One short-range communication user using multiple sDevices and wDevices	Cellular Small Cell		WiFi (sDevice, wDevice)	LTE (sDevice)		LTE (sDevice)	WiFi (sDevice, wDevice)	LTE (sDevice)	LTE (sDevice)
	Non-cellular WLAN	No WLAN			WiFi (wDevice)	No WLAN			WiFi (wDevice)
Multiple macro users & mDevices	Macrocell	LTE		LTE		LTE		LTE	

Fig. 2. Four use cases considered in this paper. Cases 1 and 2 are the baseline. Cases 3 and 4 are the focus of this paper. LTE and WiFi represent the air interfaces used in a band; blank box means the spectrum is not used. Note that in Cases 2 and 4, the sDevice can select either the cellular small cell or the non-cellular WLAN; for simplicity, we assume it always selects the cellular small cell.
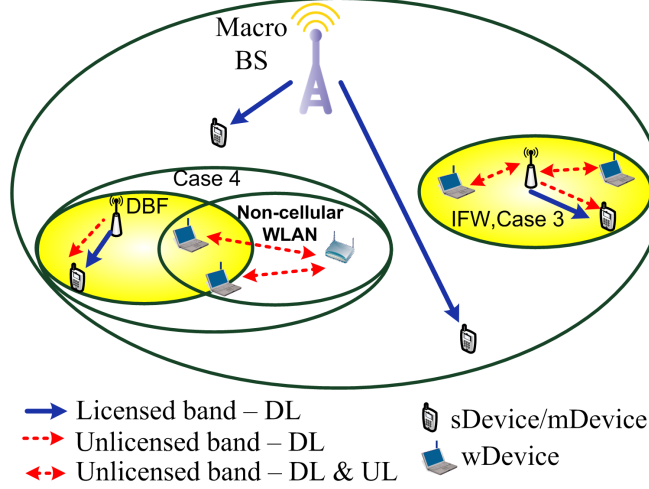

Fig. 3. Illustration of the Cases 3 and 4 scenarios considered in this paper.

II. SYSTEM MODEL

Two types of small cells, the IFW [3] introduced by the Small Cell Forum and the DBF proposed in [4] [9], that simultaneously access both licensed and unlicensed bands are considered in this paper. We consider closed access small cells that can only be accessed by registered devices [1]. In the licensed band, the LTE air interface [5], which divides the spectrum into radio blocks which are referred to as subchannels, is used. In the unlicensed band, different nodes share the air resource in time, not frequency, so we do not consider subchannels.

Throughout this paper, "WiFi hotspot," "IFW" and "DBF" refer to both the fBS and all associated devices using the appropriate radio access technology. The term "WLAN" refers to the network formed by a WiFi AP and wDevices that coexist with the sDevices in Cases 2 and 4; while the term "WiFi hotspot" refers to the small cell in Case 1 of Fig. 1 that is used by both sDevices and wDevices.

We assume that IFW and DBF BSs conduct the traffic balancing over the licensed and unlicensed bands. How to allocate radio resources (i.e., power, frequency and time) to individual *devices within one cell* in the licensed band is a complex problem [12], and is out of the scope of this paper where the focus is radio resource allocation *among different types of cells* including macrocell, small cell (IFW or DBF)

and non-cellular WLAN. Therefore, for simplicity, we only consider a single sDevice in the small cell; the extension to the multi-device small cell case could be based on an analysis similar to this paper. In addition, we assume that the licensed band and unlicensed band use separate power budgets, due to different government regulation requirements for the bands.

In the IFW use case, we consider an IFW fBS and a mBS, where the IFW fBS is connected to one sDevice and N_W wDevices and the mBS is serving N_M mDevices. Whereas in the DBF use case, we consider a DBF fBS, a WiFi AP and a mBS, where the DBF fBS is connected to one sDevice, the WiFi AP is connected to N_W wDevices, and the mBS is serving N_M mDevices. The WiFi AP may or may not be physically integrated with the DBF fBS. We consider the case where the WiFi WLAN and DBF use the same unlicensed band carrier frequency,[1] which is the worst case in terms of network performance. In either use case, the sDevice and wDevices are used by a single user or a single group of users (e.g., a family, an enterprise or passengers on the same vehicle). In the unlicensed band, the DBF fBS contends with N_W wDevices

[1]Though the bandwidth of all unlicensed band is large, typically a device only supports a limited number of the bands to lower the device cost. In dense WiFi and small cell deployments in locations such as enterprise and urban residential apartment buildings, where high interference can be observed on many unlicensed frequencies, some near-by WLANs or DBF small cells may have to use the same unlicensed band carrier frequency.

for the channel. We assume that N_W is much larger than one, and each contending node (wDevice or DBF fBS) can sense the other nodes. Furthermore, the DBF fBS success probability for each access attempt in the unlicensed band is denoted as P_{DBFsuc}. If T_{attempt} (the time interval between two channel access attempts from the DBF fBS) is comparable to the transmission durations of the other unlicensed band devices, it is reasonable to assume that the fBS channel access attempts are statistically independent.

We assume no external interference in the unlicensed band except the collisions among the transmitters in the IFW, DBF and WLAN; in case of collisions, we assume that WiFi transmissions always fail, otherwise, transmission errors are neglected since the data rate is adapted to the instantaneous SINR [13]. In addition, hidden terminal and exposed terminal problems can be detected by the DBF and IFW fBSs via existing LTE downlink channel quality indicator (CQI) feedbacks over the licensed band. In the unlicensed band, if the fBS senses good channel quality while the CQI from the UE report is constantly below a threshold, the fBS may determine that the UE is under high interference from hidden terminals. Similarly, if the fBS senses bad channel quality while the CQI from the UE report is constantly above a threshold, the fBS may determine that the fBS itself experiences exposed terminal problems. Note that the detection of hidden and exposed terminals is difficult, if not impossible, when only one unlicensed carrier frequency is used (e.g., WiFi, Bluetooth). The fBS may take different approaches upon detecting the hidden terminals, e.g., selecting another unlicensed carrier frequency to operate on, which is out of the scope of this paper.

The LTE air interface [5] supports both Frequency-Division Duplex (FDD) and Time-Division Duplex (TDD) modes. We consider FDD-mode LTE in this study. For ease of exposure, we only consider downlink transmissions for mDevices and sDevices, and assume that sDevices use the unlicensed band only for downlink transmissions in both IFW and DBF use cases (uplink is in the licensed band). For the wDevices, we consider both downlink and uplink transmissions, since the downlink contends with uplink in a random fashion and cannot be separately studied. In the unlicensed band, the performance of the sDevices in both IFW and DBF use cases is dependent on the traffic load of the coexisting wDevices, which can be described by the parameter $\bar{t}_w$, the fraction of channel time needed to deliver the UL and DL traffic of all wDevices. In general, $\bar{t}_w$ is determined by the average traffic load and data rate of every wDevice. Note that the UL and DL data rates of a wDevice are the same due to channel reciprocity. We define a wDevices throughput as the sum of uplink and downlink throughput. In order to identify the maximum capacity of the two-tiered cellular network, we assume that the mDevices and sDevices always have downlink traffic to receive (i.e., their traffic loads are more than their physical layers can support). In the licensed band, we assume that mBSs do not adjust their transmission powers in the presence of small cell interference.

Both LTE and WiFi have multiple modulation and coding schemes (MCSs) and adapt their MCSs to the instantaneous signal-to-interference-plus-noise ratios (SINRs). In practice, the WiFi rate function $R_W(\cdot)$ and LTE rate function $R_L(\cdot)$ are dependent on their MCSs and bandwidth. In this paper, we will consider the actual $R_W(\cdot)$ determined by the WiFi standard [13]. For ease of exposure, we will first conduct our analysis using Shannon capacity as $R_L(\cdot)$ in Section IV-C; then in Section IV-G, we will consider a closed-form approximation for the actual LTE rate function. It is clear that the small cell unlicensed band rate function $R_U(\cdot)$ is equal to $R_W(\cdot)$ and $R_L(\cdot)$ in IFW and DBF, respectively. We assume that the fBS knows the received SINRs at the sDevice in both licensed and unlicensed bands via device feedback. More specifically, in the licensed band, the fBS controls the transmission power $P_f^{(k)}$ and knows the received SINR $P_f^{(k)}\gamma_f^{(k)}$ of sDevice in subchannel k ($k = 1, 2, \ldots, K$). Here in subchannel k, $\gamma_f^{(k)}$ is path loss of the desired signal divided by the interference and noise power. We also assume that the fBS knows the inter-cell interference channel gain $h_{fm}^{(k)}$ ($k = 1, 2, \ldots, K$) from the fBS to the mDevice that uses subchannel k in the licensed band. For simplicity, we do not consider fading, mobility or multi-antenna transceivers, which would mainly affect the required overhead for obtaining the SINRs and channel gains in our problem formulation.

A utility function $U(S)$ is used to evaluate user satisfaction about an achieved throughput S. We will consider the widely-used logarithmic utility function to achieve proportional fairness [14],

$$U(S) = \ln(S), \tag{1}$$

where $\ln(\cdot)$ is natural logarithm function. The concavity of the logarithmic function well captures the typical user experience about throughput – as throughput increases, user satisfaction (utility) grows faster when throughput is low than when it is high.

III. A DBF CHANNEL ACCESS SCHEME FOR UNLICENSED-BAND LTE

The LTE-Advanced standard [5] introduces the carrier aggregation feature, which allows up to five component carriers (CCs) to be aggregated to form a single LTE radio interface with a bandwidth of up to 100MHz in both downlink and uplink. The CCs can be either contiguous, non-contiguous or in different bands [5]. Our proposed DBF uses the LTE air interface in both licensed and unlicensed bands via the LTE carrier aggregation feature.

LTE was designed based on the assumption of exclusive spectrum use, which is not true in the unlicensed band where devices with different air interfaces coexist. However, existing channel access schemes in the unlicensed band such as the IEEE 802.11 distributed coordination function (DCF) and point coordination function (PCF) [13], are not designed for cellular air interfaces, and do not align with the LTE frame structure. LTE transmissions are organized in periodic subframes in time, and can start only at the beginning of subframes [5]. As a result, channel access attempts in the unlicensed band must take place right before the start time of subframes. Otherwise, even though the fBS obtains the channel, it cannot transmit until the start time of the next
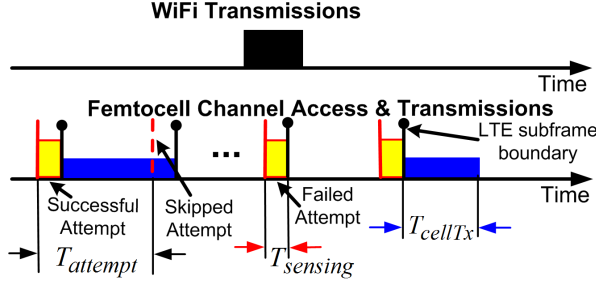
Fig. 4. Dual-Band Femtocell (DBF) channel access mechanism in the unlicensed band.

subframe, and may lose the transmission opportunity since other unlicensed-band devices will find the channel idle and transmit. Therefore, in this section, we propose a channel access scheme that aligns with LTE frame structure. Once the access to the unlicensed band is obtained, the fBS will follow the standard LTE air interface and assign radio resources to the sDevices through the licensed-band control channel.

Two guidelines are followed in the design of the DBF channel access scheme for the unlicensed band: 1) The fBS senses the unlicensed spectrum in order to avoid interference from ongoing transmissions by other unlicensed-band devices. 2) The channel access scheme aligns with LTE frame structure.

Fig. 4 illustrates the proposed channel access scheme. The fBS attempts to access the channel at pre-assigned periodic time instants, called "access opportunities." The period of the access opportunities is denoted as T_{attempt}. At each access opportunity, the fBS senses the unlicensed band, which takes T_{sensing} seconds. If the channel is idle, the fBS will access the channel and use it for a fixed duration, T_{cellTx}; otherwise, the fBS will wait for the next access opportunity.

As shown in Fig. 4, to fit this channel access scheme with the periodic LTE subframe structure, we require both T_{attempt} and T_{cellTx} should be integer multiples of LTE subframe duration which is 1ms [5]. Also, the T_{attempt} includes the T_{sensing} and the access opportunity must be T_{sensing} before the LTE subframe boundary so that the fBS can complete sensing the unlicensed band right at the LTE subframe boundary and transmit using the whole LTE subframe. Moreover, As we will see in Sec. VI, a DBF fBS can adjust its unlicensed band usage by tuning the parameters T_{attempt} and T_{cellTx}. In practice, the channel sensing time T_{sensing} is mainly determined by the hardware and is on the order of 10 microseconds [13] which is far less than the T_{attempt} and T_{cellTx}, therefore having negligible impact to DBF performance.

In order to prevent DBFs from keeping the channel for a long time, the fBS should not access the channel immediately after a channel use. If the end of a transmission happens to be an access opportunity, the fBS should skip it; if the end of a transmission is in between two access opportunities, the fBS should skip the access opportunity immediately following the end of the transmission. This guarantees that the DBF leaves at least T_{attempt} seconds between two consecutive transmissions for other coexisting devices to access the unlicensed band.

IV. SMALL CELL TRAFFIC BALANCING OVER LICENSED AND UNLICENSED BANDS

In this section, we formulate a traffic balancing strategy for dual-band small cells in Cases 3 and 4 of Fig. 2 to assign traffic over the licensed and unlicensed bands. The formulation is independent of the unlicensed band RAT, hence applicable to both IFW and DBF; whereas the implementation will be RAT-dependent and will be described in Sec. V for IFW and in Sec. VI for DBF.

A. Transmission Parameters for Traffic Balancing

The IFW and DBF access the unlicensed band based on channel sensing, so at most one device can use the channel at any given time, except for collisions. Hence, the unlicensed band is shared in time among different devices, and the unlicensed-band usage can be best characterized by the fraction of time that a device occupies the channel. We will control small cell unlicensed-band usage by tuning its fraction of channel time t_f, which will impact t_w, the total fraction of channel time used by all the wDevices. The licensed band is simultaneously utilized by all small and macro cells, and some mDevices may experience severe interference from small cells [2]. We will adjust fBS transmission power $P_f^{(k)}$ in subchannel k, so that the interference to mDevices can be controlled, while the desired performance for sDevices is obtained.

B. Downlink User Utility Optimization for DBF and IFW Use Cases

Recall that in the system model in Section II, for both DBF and IFW small cells, there is an sDevice and N_W wDevices which are used by a single user or single group of users. The sDevice shares the unlicensed band with N_W wDevices and the licensed band with N_M mDevices. The buffer status (e.g., full-buffer or not) of the wDevices depends on not only their aggregate load $\bar{t}_w$, but also the DBF or IFW cell's channel time usage t_f. For example, if $\bar{t}_w = 50\%$, the wDevices will not be in full-buffer status when there is no other unlicensed band user; however, in the DBF and IFW scenarios where $t_f = 60\%$, the wDevices will be in full-buffer status. Recall that the sDevices always have traffic to receive, so the optimal t_f should be such that

$$t_{max} - t_f \le \bar{t}_w \tag{2}$$

where t_{max} is the maximum fraction of time that the unlicensed band can be used;[2] otherwise, part of the available unlicensed band channel will be unused, resulting in suboptimality. Consequently, with optimal traffic balancing in the DBF or IFW cells, the wDevices will always be in full buffer status [15], although their traffic loads may be limited.

It has been shown in [16]–[18] that for a WLAN with full-buffer stations and no other unlicensed band users, WLAN station i's fraction of channel time α_i is determined by

---

[2]The t_{max} is determined by the channel access schemes in the unlicensed band, and is strictly less than one if channel-sensing based access schemes are used. If $t_{max} = 1$, then the unlicensed-band channel is always being used and all devices will detect channel busy and not access the channel, which contradicts the assumption $t_{max} = 1$.

the channel access parameters and channel conditions of all stations. Hence, in DBF or IFW use case with optimal traffic balancing, the transmission time $t_{w,i}$ of wDevice i (in terms of fraction of the whole channel time) is

$$t_{w,i} = \alpha_i t_w, \quad i = 1, 2, \ldots, N_W, \tag{3}$$

where t_w is the channel usage of all N_W wDevices. Then the throughput of a wDevice is

$$S_{W,i} = R_{W,i} t_{w,i} = R_{W,i} \alpha_i t_w, \ i = 1, 2, \ldots, N_W, \tag{4}$$

where $R_{W,i}$ is determined by WiFi rate function $R_W(\cdot)$ and device i's instantaneous SINR. In Section IV-C, we show that α_i has no impact to the final optimal solution.

The throughput of the sDevice is from both the licensed and unlicensed bands. In the licensed band, the sDevice and mDevices simultaneously use the band, so power control is needed to keep the interference from the fBS to the mDevices below given thresholds. In the unlicensed band, the "listen before talk" style of channel access is widely used (e.g., WiFi), so interference is not a major issue, hence we do not apply power control. Recall that the fBS knows downlink SINR via device feedback, in addition, the licensed and unlicensed bands use separate power budgets due to different government regulation requirements, so the unlicensed band data rate R_U is a constant that is determined by WiFi rate function $R_W(\cdot)$ (for IFW), LTE rate function $R_L(\cdot)$ (for DBF) and the instantaneous SINR in the unlicensed band. The unlicensed band channel is shared by sDevices and wDevices in time, so we control the fraction of channel time t_f that is used by the sDevice. Then the sDevice throughput is

$$S_f = \sum_k R_L(P_f^{(k)} \gamma_f^{(k)}) + t_f R_U, \tag{5}$$

where $P_f^{(k)}$ is the transmission power in subchannel k of the licensed band.

The optimization problem can be formulated as,

$$\max_{P_f^{(k)}, \, t_f, \, t_w} \quad U_{sum} = \sum_{i=1}^{N_W} U(R_{W,i} \alpha_i t_w) \; +$$

$$U\left(\sum_k R_L(P_f^{(k)} \gamma_f^{(k)}) + t_f R_U\right), \tag{6}$$

$$\text{Subject to} \quad P_f^{(k)} |h_{fm}^{(k)}|^2 \le \bar{I}_k, \ k = 1, 2, \ldots, K, \tag{7}$$

$$t_f + t_w \le t_{max}, \tag{8}$$

$$t_w \le \bar{t}_w \tag{9}$$

$$\sum_k P_f^{(k)} \le P_{tot}, \tag{10}$$

$$t_f \ge 0, t_w \ge 0, P_f^{(k)} \ge 0, \ k = 1, 2, \ldots, K. \tag{11}$$

Constraint (7) follows the widely-adopted principle [2] in two-tiered networks which requires that the interference power leaked from the small cell to the macrocell cannot exceed the maximum allowed interference temperature $\bar{I}_k$ in subchannel k ($k = 1, 2, \ldots, K$), which are predefined system parameters that determine the performance tradeoff between macro and

small cells in the licensed band. Constraint (8) shows the fact that, in practice, the total unlicensed band usage must be less or equal to the maximum fraction of time t_{max} that the unlicensed band can be used. Constraint (9) specifies that the aggregate wDevice channel usage cannot exceed the time determined by their aggregate traffic load.

For the convenience of presentation, we treat t_w as a variable for the fBS to optimize in the problem formulation above; however, the final solution in Section IV-C shows that the fBS does not need to adjust t_w – whenever the fBS adjusts its t_f, the t_w is automatically adjusted. The objective (6) maximizes the total user experience/utility from all the sDevice and wDevices used by the user (or group of users), and is equivalent to

$$\max_{P_f^{(k)}, \, t_f, \, t_w} \quad U\left(\sum_k R_L(P_f^{(k)} \gamma_f^{(k)}) + t_f R_U\right) + N_W U(t_w). \tag{12}$$

The mathematical formulation (6)-(11) shares some similarities with the optimization problem in [2]; however, unlike [2] which only considers the licensed band, our optimization considers traffic balancing over both licensed and unlicensed bands.

C. Solution to the Optimization Problem

In the above optimization problem, $P_f^{(k)}$ affects the sum utility (6) only through the small cell licensed-band throughput $\sum_k R_L(P_f^{(k)} \gamma_f^{(k)})$. In addition, the utility function $U(S) = \ln(S)$ is strictly increasing with throughput S, hence maximizing small cell licensed-band throughput $\sum_k R_L(P_f^{(k)} \gamma_f^{(k)})$ subject to (7) and (10) will optimize the sum utility (6) as well. Therefore, to find the optimal $P_f^{(k)}$, we solve the following optimization problem,

$$\max_{P_f^{(k)}} \quad \sum_k R_L(P_f^{(k)} \gamma_f^{(k)}) \tag{13}$$

$$\text{Subject to} \quad \sum_k P_f^{(k)} \le P_{tot}, \tag{14}$$

$$0 \le P_f^{(k)} \le \bar{I}_k / |h_{fm}^{(k)}|^2, \ k = 1, 2, \ldots, K. \tag{15}$$

After obtaining the optimal $P_f^{*(k)}$, finding the optimal t_f to the original optimization problem (6)-(11) is equivalent to the following,

$$\max_{t_f, \, t_w} \quad U\left(\sum_k R_L(P_f^{*(k)} \gamma_f^{(k)}) + t_f R_U\right) +$$

$$N_W U(t_w), \tag{16}$$

$$\text{Subject to} \quad t_f + t_w \le t_{max}, \tag{17}$$

$$t_f \ge 0, \quad 0 \le t_w \le \bar{t}_w. \tag{18}$$

We first consider the optimization in (13)-(15). In this subsection we solve the problem assuming that the rate function $R_L(\cdot)$ is given by Shannon capacity, that is

$$R_L(P_f^{(k)} \gamma_f^{(k)}) = B \log_2(1 + P_f^{(k)} \gamma_f^{(k)}), \tag{19}$$

where B is the bandwidth of a small cell subchannel in the licensed band. In Section IV-G we will discuss how this analysis can be extended to the case when $R_L(\cdot)$ is obtained using an approximation to the LTE rate function. Using the Karush-Kuhn-Tucker (KKT) conditions [19], it is easy to see that the solution to (13)-(15) with $R_L(\cdot)$ defined in (19) is given by

$$P_f^{*(k)} = \min\left(\left(\frac{1}{\mu} - \frac{1}{\gamma_f^{(k)}}\right)^+, \frac{\bar{I}_k}{|h_{fm}^{(k)}|^2}\right), \qquad (20)$$

Here $x^+ = \max(0, x)$, and μ is chosen to satisfy (14) with equality. The solution in (20) can be numerically obtained by the *modified water-filling algorithm* [20] [21], which allocates power into subchannels similar to regular water-filling procedure, with the only difference that the power in subchannel k must be below $\bar{I}_k / |h_{fm}^{(k)}|^2$.

Based on the optimal $P_f^{*(k)}$ obtained above, we next solve the second optimization problem (16)-(18). Since $P_f^{*(k)}$ has been determined, the total LTE licensed band rate of the sDevice,

$$R_L^{tot} = \sum_k R_L(P_f^{*(k)} \gamma_f^{(k)}), \qquad (21)$$

is now a constant. The objective function (16) is an increasing function of t_f and t_w (recall that $U(\cdot) = \ln(\cdot)$), so equality must be achieved in Constraint (17) to maximize (16), hence we have

$$t_w = t_{max} - t_f. \qquad (22)$$

Submit (21) and (22) into the optimization problem (16)-(18), we obtain the simplified formulation below,

$$\max_{t_f} \quad \ln(t_f + R_L^{tot}/R_U) + N_W \ln(t_{max} - t_f) \quad (23)$$

$$\text{Subject to} \quad t_f \geq 0, \quad 0 \leq t_w \leq \bar{t}_w. \qquad (24)$$

We temporarily ignore the Constraint (24), take the derivative of (23) with respect to t_f and set the derivative to zero, we can see that

$$t_f^* = \frac{1}{N_W + 1}\left(t_{max} - N_W \frac{R_L^{tot}}{R_U}\right). \qquad (25)$$

Then we consider the Constraint (24) which defines the fixed traffic load of the wDevices, from which we have

$$t_f^* \geq (t_{max} - \bar{t}_w)^+, \qquad (26)$$

because sDevices always have data to receive; otherwise, part of the available unlicensed band channel will be unused which results in suboptimal t_f^*. Therefore,

$$
\begin{aligned}
t_f^* &= \max\left(\frac{1}{N_W + 1}\left(t_{max} - N_W \frac{R_L^{tot}}{R_U}\right)^+, \right. \\
&\qquad\qquad (t_{max} - \bar{t}_w)^+ \,) \\
&= \max\left(\ (t_{max} - \bar{t}_w)^+ \ , \right. \\
&\qquad \left. \frac{1}{N_W + 1}\left(t_{max} - N_W \frac{\sum_k R_L(P_f^{*(k)} \gamma_f^{(k)})}{R_U}\right)^+\right)
\end{aligned}
$$
$$(27)$$

$$t_w^* = t_{max} - t_f^*. \qquad (28)$$

The solution (28) shows that the fBS can control the wDevice channel usage t_w by adjusting the sDevice channel usage t_f.

The fBS will compute the optimal transmit power $P_f^{*(k)}$ in the licensed band and the optimal transmission time t_f^* in the unlicensed band using (20) and (27), respectively. The fBS will then adjust the amount of traffic assigned to the unlicensed band so that it transmits in the unlicensed band for t_f^* fraction of time. The fBS will assign the rest traffic to the licensed band. In addition, the fBS will transmit at a power of $P_f^{*(k)}$ in subchannel k of the licensed band. Note that although wDevice data rate R_W appears in our problem formulation (6), it does not appear in the final solutions of $P_f^{*(k)}$ and t_f^*. As a result, the fBS does not have to obtain wDevice data rate information to carry out the optimal traffic-balancing scheme.

D. Intuitions Behind the Optimal Solution

In this subsection, we discuss the intuitions behind the optimal t_f solution.

Case H1: Firstly, we consider a high wDevice load case where

$$\bar{t}_w \geq t_{max} \qquad (29)$$

and

$$N_W R_L^{tot}/R_U \leq t_{max} \qquad (30)$$

are both satisfied. From (27) and (28) we have

$$
\begin{aligned}
t_f^* &= \frac{1}{N_W + 1}\left(t_{max} - N_W \frac{R_L^{tot}}{R_U}\right), \\
t_w^* &= \frac{N_W}{N_W + 1}(t_{max} + R_L^{tot}/R_U).
\end{aligned}
$$
$$(31)$$

The sDevice throughput is from both the licensed and unlicensed band. We can translate the total sDevice throughput into the unlicensed band channel time t_f' as if the licensed band throughput were also obtained from the unlicensed band,

$$t_f' = \frac{R_L^{tot} + t_f^* R_U}{R_U} = \frac{t_{max} + R_L^{tot}/R_U}{N_W + 1}. \qquad (32)$$

As we can see,

$$t_f' = \frac{t_f' + t_w^*}{N_W + 1}. \qquad (33)$$

Therefore, when the conditions (29) and (30) are both satisfied, the optimization process *effectively translates the total sDevice throughput (of licensed and unlicensed bands) into the unlicensed band channel time t_f'*, and guarantees that t_f' is an *equal share of the combined channel time* $(t_f' + t_w^*)$. An extreme case of the condition (30) is

$$N_W R_L^{tot}/R_U \ll t_{max}, \qquad (34)$$

then we can obtain

$$t_f^* \approx \frac{t_{max}}{N_W + 1}, \qquad (35)$$

$$t_w^* \approx \frac{N_W t_{max}}{N_W + 1}. \qquad (36)$$

From (35) and (36), we further confirm that the optimization process assigns an equal share of the unlicensed band channel time to the sDevice.
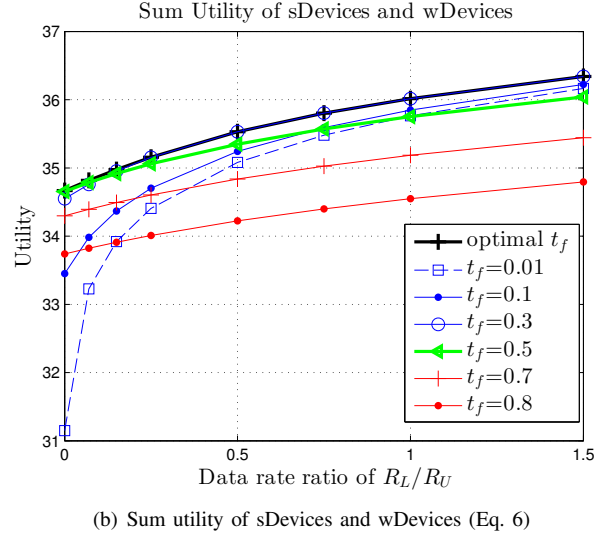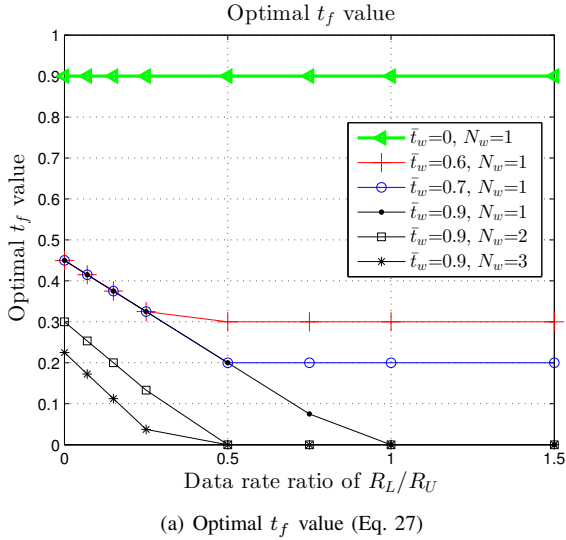
(a) Optimal t_f value (Eq. 27)

(b) Sum utility of sDevices and wDevices (Eq. 6)

Fig. 5. Optimal small cell usage, t_f, and sum utility as functions of R_L^{tot}/R_U. Different ratios of R_L^{tot}/R_U are obtained by varying licensed bandwidth (1.4, 3, 5, 10, 15, 20 and 30 MHz). $t_{max} = 0.9$. Fig. 5(b) further assumes $N_w = 1$ and $\bar{t}_w = 0.6$.

Case H2: If (29) is satisfied (i.e., high wDevice load) and (30) is not, we can get $t_f^* = 0$ from (27). Similar to Case H1, the optimization process in this case still translates the total sDevice throughput into the unlicensed band channel time t_f', but R_L^{tot}/R_U is so large that we can never achieve $t_f' = (t_f' + t_w^*)/(N_W + 1)$. The best solution is $t_f^* = 0$ which minimizes the difference between t_f' and $(t_f' + t_w^*)/(N_W + 1)$.

Case L1: We consider a low wDevice load case where the following is satisfied

$$\bar{t}_w \leq N_W \frac{t_{max} + R_L^{tot}/R_U}{N_W + 1}. \tag{37}$$

The optimal solution t_f in (27) can be simplified to,

$$t_f^* = (t_{max} - \bar{t}_w)^+. \tag{38}$$

In this case since the wDevice aggregate traffic load is limited, the sDevice tries to use the remaining available channel time.

E. Numerical Results

Fig. 5(a) shows the numerical results of Eq. (27) under different ratios of R_L^{tot}/R_U. In Figures 5(a) and 5(b), we assume that $P_f^{*(k)}$ and $\gamma_f^{(k)}$ values are such that sDevices have fixed spectral efficiency 3.9 bits/second/Hz for licensed and unlicensed bands, hence only the licensed and unlicensed bandwidth affects R_L^{tot} and R_U, respectively. We fix unlicensed bandwidth to 20MHz, and vary licensed bandwidth (1.4, 3, 5, 10, 15, 20 and 30 MHz) to obtain different instantaneous licensed band rate R_L^{tot}'s. The LTE licensed carrier frequency bandwidth can only be up to 20MHz; the 30MHz is due to carrier aggregation of multiple licensed carrier frequencies. The highest rate 72Mbps is used for the wDevice physical layer data rate R_W.

Fig. 5(b) shows the numerical results of sum utility in Eq. (6) with respect to t_f. Here we assume $N_w = 1$ and $\bar{t}_w = 0.6$. From Fig. 5(a) we see that the optimal t_f depends on many parameters. In this figure, we observe that a constant t_f cannot achieve good sum utility under every condition. Note that constant $t_f = 0.3$ achieves almost the optimal sum utility, which is because it is close to the optimal t_f range [0.3, 0.45] (see Fig. 5(a)). Since we use fixed spectral efficiency for the licensed band, the utility gain in the figure is only from t_f optimization, not power control. Therefore, while the existing studies [2] show that licensed band power control is very useful for small cells, this figure suggests that when power control has been done for the licensed band, we can further improve user utility by time-sharing control of t_f in the unlicensed band. In addition, we also observe that the utility increases as t_f becomes closer to the optimal value. We study the impact of the sum utility sensitivity to the change of t_f in Section IV-F.

F. Sensitivity Analysis

In this subsection, we analyze the impact of t_f to the sum utility U_{sum} formulated in (6). Unlike the optimization analysis in the previous subsection, the t_f assignment in this subsection may not be optimal, hence we do not assume $t_f + t_w = t_{max}$ here. We consider two cases based on the t_f value.

Case A: If condition (39) is satisfied,

$$t_{max} - t_f \leq \bar{t}_w , \tag{39}$$

we have

$$t_w = t_{max} - t_f. \tag{40}$$

Plugging (40) into the sum utility (6) and taking the derivative of U_{sum} with respect to t_f, we obtain the first order approximation to the sum utility change ΔU_{sum} when t_f is increased to $(t_f + \Delta t_f)$,

$$\Delta U_{sum} = \left(\frac{1}{(\sum_k R_L(P_f^{(k)} \gamma_f^{(k)}))/R_U + \tilde{t}_f} - \frac{N_W}{t_{max} - \tilde{t}_f} \right) \Delta t_f. \tag{41}$$
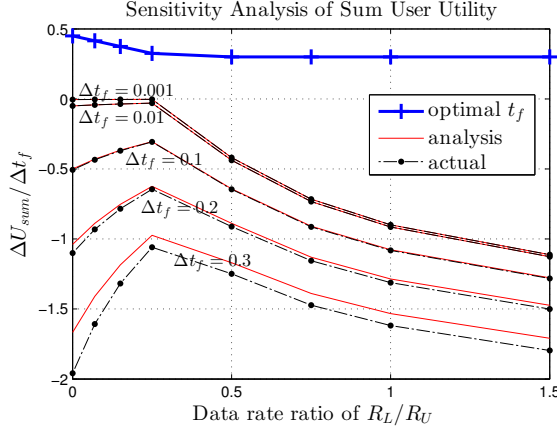
Fig. 6. Sensitivity of sum utility to variations in t_f based on $N_w = 1$, $\bar{t}_w = 0.6$ and optimal t_f^*. Note that the Y-axis is $\Delta U_{sum}/\Delta t_f$. The "analysis" curves are obtained from (41) and (43). The "actual" curves are obtained from (6) by calculating $(U_{sum}(t_f^* + \Delta t_f) - U_{sum}(t_f^*))/\Delta t_f$.

Here we use the middle point $\tilde{t}_f = t_f + \Delta t_f/2$ to improve the approximation.

Case B: If condition (39) is not satisfied, we have

$$t_w = \bar{t}_w. \tag{42}$$

Submit (42) into the sum utility (6) and take the derivative of U_{sum} with respect to t_f, we obtain

$$\Delta U_{sum} = \left(\frac{1}{(\sum_k R_L(P_f^{(k)} \gamma_f^{(k)}))/R_U + \tilde{t}_f} \right) \Delta t_f, \tag{43}$$

where $\tilde{t}_f = t_f + \Delta t_f/2$.

Fig. 6 shows the numeric results of the above analysis. The "actual" curves are obtained from (6) by calculating $(U_{sum}(t_f^* + \Delta t_f) - U_{sum}(t_f^*))/\Delta t_f$. The "analysis" curves are obtained from (41) and (43). We observe that the sum utility degrades as t_f deviates more from the optimal value, which is consistent with the observation in Fig. 5(b). For negative Δt_f values, we observe similar trend of sum utility degradation, which is not shown here.

G. Implementation Issues

The analysis in Section IV-C considered Shannon capacity as the rate function $R_L(\cdot)$. For practical LTE networks, Mogensen et al. [22] propose a closed-form approximation for the LTE rate function,

$$R_L(\text{SINR}) \approx \kappa_{bw} \cdot \kappa_c \cdot B \log_2(1 + \text{SINR}/\kappa_{sinr}) \text{ bits/s}, \tag{44}$$

where κ_{bw} is the system efficiency that accounts for various system-level overheads including cyclic prefix, pilot assisted channel estimation, and non-fully utilized frequency bandwidth (to prevent signal leakage to adjacent frequencies). The parameters κ_c and κ_{sinr} jointly adjust for the SINR implementation efficiency of LTE MCSs and receiver algorithms (e.g., linear, non-linear) [22]. The value of κ_{bw} can be directly derived from LTE protocol parameters, whereas κ_c and κ_{sinr} can be obtained by fitting the LTE rate curve generated from link-level simulations. For a realistic implementation of the

traffic balancing strategy, the analysis in Section IV-C can be replicated by using the $R_L(\cdot)$ in (44). In our simulations, we will approximate SISO LTE-A rates using $\kappa_{bw} = 0.6726$, $\kappa_c = 0.75$ and $\kappa_{sinr} = 1$ in (44).

Another implementation issue is that the proposed algorithm requires the fBS to know the channel gain $|h_{fm}^{(k)}|$ of the fBS-to-mDevice interference link, as required by the constraint (7). In current cellular networks, exact value of $|h_{fm}^{(k)}|$ may be difficult to obtain. However, this problem will be addressed in the future, based on the current developments in LTE-A. For example, the 3GPP is investigating macro-Femto coordination mechanisms [23]. Based on the mechanism proposed in [23, Sec. 7.2.2.6.2], one can further estimate $|h_{fm}^{(k)}|$ based on path loss. For beyond-4G cellular systems, [24] proposes that the mBS broadcasts mDevice locations and the resources used by each mDevice, so that femtocells/small cells can estimate the $|h_{fm}^{(k)}|$ according to the fBS-to-mDevice distances. In our simulations, we will assume $|h_{fm}^{(k)}|$ is known at the fBS.

The fBS also needs to know the traffic load $\bar{t}_w$ of the wDevices, which is the aggregate DL and UL channel time used by the wDevices before the sDevice uses the unlicensed band, and can be obtained via fBS long-term sensing.[3] In addition, the fBS also needs to learn N_W, the number of coexisting wDevices. The IFW fBS can learn N_W from the MAC addresses of the wDevices; whereas the DBF fBS can learn N_W using the RF fingerprint technique [25] which allows the fBS to distinguish each transmitter based on their unique radio characteristics (or "RF fingerprint") without decoding their signals.

V. Adjusting Unlicensed Band Usage for sDevice in Integrated Femto-WiFi

The optimal traffic-balancing scheme introduced in Section IV requires the fBS to adjust t_f, the fraction of time the fBS transmits in the unlicensed band to the sDevice. In this section, we discuss how this can be done for the IFW use case; in Section VI, we will study the DBF use case.

Recall that in the IFW use case, the fBS contends with N_W wDevices for the same channel. In addition, the fBS transmits to both sDevice and wDevices. The total fBS channel time is

$$t_{fBS} = t_f + t_w^{dl}, \tag{45}$$

where t_w^{dl} is the DL channel time for all wDevices. When $t_w = \bar{t}_w$, t_w^{dl} is the time required to transmit the DL traffic load of all wDevices. When $t_w < \bar{t}_w$, t_w^{dl} is a predefined fraction of t_w; in this paper, we assume t_w^{dl} is proportional to the DL traffic load $\bar{t}_w^{dl}$,

$$t_w^{dl} = \frac{\bar{t}_w^{dl}}{\bar{t}_w} t_w. \tag{46}$$

Once the fBS obtains t_{fBS} channel time, it assigns t_f to the sDevice and t_w^{dl} to the wDevices.

---

[3]Since the IFW fBS is connected to both sDevice and wDevices and the wDevices have both downlink and uplink traffic, the fBS transmission is split between the sDevice and wDevices. Therefore, the $\bar{t}_w$ measurement in IFW cell should take into account the DL transmission from the fBS to the wDevices and the UL transmission from the wDevices.

Studies such as [26] have shown that WiFi channel usage in the unlicensed band is a monotonically decreasing function of its initial backoff window size. Therefore, we can adjust the fBS channel usage t_{fBS} in the unlicensed band by tuning the fBS initial backoff window size W_f. However, directly using the analytical result [26] in practice requires the knowledge of the initial backoff window sizes and the transmission durations of the wDevices, which are possible via the feedback from the wDevice to the IFW fBS. However, such feedback is not supported by existing WiFi protocol. Therefore, to ensure that our algorithm works for existing WiFi technologies, we developed the bisection-based Algorithm 1 which only uses *the trend that the fBS channel usage t_{fBS} in the unlicensed band is a monotonic function of its initial backoff window size W_f.* The monotonicity of the $t_{fBS}(W_f)$ function makes it appropriate to use bisection [27] to efficiently search for the W_f that can achieve a given t_{fBS}. The bisection algorithm needs to know the channel usages for some window size values, which can be obtained through measurements. The fBS first sets its parameter W_f to the window size value that needs to be measured, and utilizes the channel for a certain time. During this time, the fBS periodically records its transmission state (idle or transmitting) at each sampled time instant. We denote N_{tot} as the total number of time samples, out of which N_{tx} samples turn out that the fBS is transmitting. Then the measured t_{fBS} is

$$t_{fBS} = N_{tx}/N_{tot}, \quad (47)$$

The measurements can be implemented in software and do not require any additional hardware. Algorithm 1 is guaranteed to converge to the desired W_f^* and t_{fBS}^* by [27].

Algorithm 1 Find the desired W_f^* for IFW to obtain channel usage $t_{fBS}^* = t_f^* + t_w^{dl}$

1: Initialize W_f range $[W_f^{(1)}, W_f^{(2)}]$, such that $t_{fBS}^* \in [t_{fBS}(W_f^{(2)}), t_{fBS}(W_f^{(1)})]$.
2: **repeat**
3:     Set $W_f = (W_f^{(1)} + W_f^{(2)})/2$ and measure t_{fBS}.
4:     **if** $(t_{fBS}(W_f) - t_{fBS}^*)(t_{fBS}(W_f^{(1)}) - t_{fBS}^*) > 0$ **then**
5:         Set $W_f^{(1)} = W_f$.
6:     **else**
7:         Set $W_f^{(2)} = W_f$.
8:     **end if**
9: **until** $|t_{fBS}(W_f) - t_{fBS}^*| <$ tolerance

VI. Adjusting Unlicensed Band Usage for Dual-Band Femtocell

In this section, we discuss how t_f can be adjusted for the DBF which uses the access scheme introduced in Section III.

A. DBF Channel Usage Analysis

We first describe an analytical model to obtain t_f in DBF. In the unlicensed band, the DBF fBS contends with N_W wDevices and one WiFi AP for the channel. Recall that we denote the network formed by the wDevices and the AP

as "WLAN". According to the channel access scheme in Section III, in a channel access attempt, if the channel is successfully obtained, the fBS transmits for a fixed duration T_{cellTx}; otherwise, it will attempt again after a fixed time duration $T_{attempt}$. The success probability for each attempt is denoted as P_{DBFsuc}. Recall that the fBS channel access attempts are statistically independent. As such, $1/P_{DBFsuc}$ attempts are needed on average for the fBS to obtain the channel. Considering $T_{sensing} \ll \min(T_{cellTx}, T_{attempt})$, the fraction of channel time occupied by the small cell is

$$t_f = \frac{T_{cellTx}}{(1/P_{DBFsuc}) \cdot T_{attempt} + T_{cellTx}} = \frac{\eta}{1/P_{DBFsuc} + \eta}, \quad (48)$$

where

$$\eta = T_{cellTx}/T_{attempt}.$$

As we can see from (48), to find t_f, we need to know the attempt success probability P_{DBFsuc} which will be obtained in the following.

WiFi nodes (wDevices or AP) access the channel in a random fashion, resulting in random channel states (idle, collision, or successful transmission) at any given time. The fractions of time that WiFi channel is idle, in collision state and in successful transmission state, are mainly determined by transmission buffer status, number of contenders and exponential backoff parameters. Recall that under the proposed traffic-balancing scheme in Sec. IV, the wDevices will always have data to send, although its traffic load may be limited. In addition, since there are many wDevices, the introduction of a fBS increases the number of contenders by a small fraction. Hence, the WLAN has almost the same fractions of idle, collision and successful transmission time, respectively, in the WLAN/DBF cell coexistence scenario as in the full-buffer WLAN-only scenario.

The fraction of idle channel time in a full-buffer WLAN-only network can be obtained by using a 2D Markov chain to analyze the WLAN exponential backoff process, as done in [16]–[18]. Foh and Tantra's analysis [17] show that the probabilities for a WLAN channel to be in idle, collision and successful transmission states are related to the previous channel state. Given that the previous channel state is busy (i.e., successful transmission or collision), the conditional probabilities for these three states are P_I, P_c and P_s, respectively. Given that the previous channel state is idle, the conditional probabilities for these three states are Q_I, Q_c and Q_s, respectively. These probabilities can be obtained using the analytical results in [17] (see equations (2)-(5) in [17]).

When the channel is busy, every WLAN node (wDevice or AP) freezes its backoff counter and waits until the channel becomes idle. Then each node will defer for a fixed duration named DCF Interframe Space (DIFS) before resuming counting down its backoff counter in every idle backoff slot. The nodes that hit zero will transmit and the other ones will freeze their counters. A transmission may be successful or collided. As illustrated by Fig. 7, we denote a *super slot* (SS) as a WLAN time period consisting of a DIFS, i $(i = 0, 1, 2, \dots)$ consecutive idle backoff time slots, and a busy channel state. The WLAN channel is constituted by consecutive SS's, so
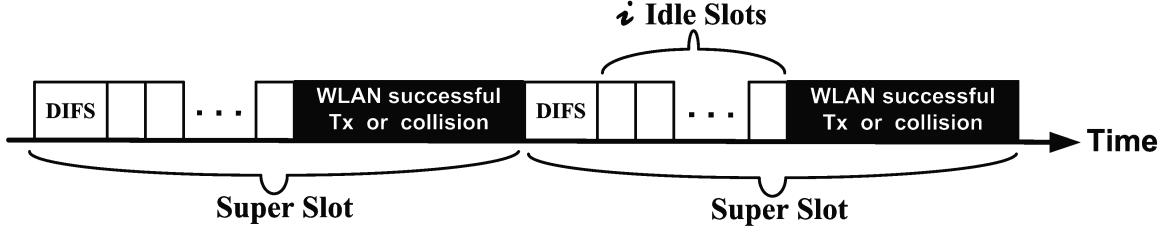
Fig. 7. WLAN channel can be viewed as consisting of consecutive super slots.

an fBS attempt time instant is randomly located in one of the SS's. We denote $SS_{i,u}^{(s)}$ as an SS with i consecutive idle slots and a successful transmission from or to device u. We also denote $SS_i^{(c)}$ as an SS with i consecutive idle slots and a collided transmission. Since each WLAN node has an equal number of transmissions [28], given that the previous channel state is busy, the probability that we have a successful transmission from device u is P_s/N_W. Similarly, given that the previous channel state is idle, the probability that we have a successful transmission from device u is Q_s/N_W. Hence, the probability of observing $SS_{i,u}^{(s)}$ is

$$P_{i,u}^{(s)} = \begin{cases} P_s/N_W, & \text{if } i = 0; \text{ and} \\ P_I Q_I^{i-1} Q_s/N_W, & \text{if } i = 1, 2, \ldots. \end{cases} \quad (49)$$

Likewise, the probability for $SS_i^{(c)}$ to happen is

$$P_i^{(c)} = \begin{cases} P_c, & \text{if } i = 0; \text{ and} \\ P_I Q_I^{i-1} Q_c, & \text{if } i = 1, 2, \ldots. \end{cases} \quad (50)$$

Further denoting the durations of a DIFS, an idle backoff slot, a collision and a successful transmission from device u ($u = 1, 2, \ldots, N_W$), as T_d, T_I, T_c and $T_{s,u}$, respectively, the durations of $SS_{i,u}^{(s)}$ and $SS_i^{(c)}$ are

$$T_{i,u}^{(s)} = T_d + iT_I + T_{s,u} \quad \text{and} \quad (51)$$
$$T_i^{(c)} = T_d + iT_I + T_c, \quad \text{respectively.} \quad (52)$$

Here $T_{s,u}$ is a constant that mainly depends on the payload length and data rate of device u, as well as various protocol overheads such as RTS/CTS/ACK messages. The constants T_d and T_I are defined in IEEE 802.11 standards. The expected duration of an SS is

$$\begin{aligned} T_{\text{avg}} &= \sum_{i=0}^{\infty} P_i^{(c)} T_i^{(c)} + \sum_{i=0}^{\infty} \sum_{u=1}^{N_W} P_{i,u}^{(s)} T_{i,u}^{(s)} \\ &= T_d + \frac{P_I T_I}{1 - Q_I} + T_c \left(P_c + \frac{Q_c P_I}{1 - Q_I} \right) + \\ &\quad \frac{\sum_u T_{s,u}}{N_W} \left(P_s + \frac{Q_s P_I}{1 - Q_I} \right). \end{aligned} \quad (53)$$

Therefore, the probability that an fBS attempt time is located in an $SS_i^{(c)}$ and $SS_{i,u}^{(s)}$ are respectively

$$\tilde{P}_i^{(c)} = \frac{P_i^{(c)} T_i^{(c)}}{T_{\text{avg}}} \quad \text{and} \quad \tilde{P}_{(i,u)}^{(s)} = \frac{P_{(i,u)}^{(s)} T_{i,u}^{(s)}}{T_{\text{avg}}}. \quad (54)$$

We denote i_0 as the minimum number of idle slots that a $SS_{i,u}^{(s)}$ must have in order to provide a long enough idle period so that an fBS channel sensing may be successful,

$$i_0 = \left\lceil \frac{T_{\text{sensing}} - T_d}{T_I} \right\rceil^+. \quad (55)$$

Here $\lceil x \rceil^+$ denotes the smallest non-negative integer that is greater than or equal to x. Given that an fBS attempt time instant is located in an $SS_i^{(c)}$ and $i \geq i_0$, the conditional probability that the fBS attempt is successful is

$$P_{\text{Suc},i}^{(c)} = \frac{T_d + iT_I - T_{\text{sensing}}}{T_i^{(c)}}, \quad (56)$$

which is also the conditional probability that the channel is idle for at least T_{sensing} time after a DBF attempt time instant. Likewise, given that an fBS attempt is in an $SS_{i,u}^{(s)}$ and $i \geq i_0$, the conditional fBS attempt success probability is

$$P_{\text{Suc},(i,u)}^{(s)} = \frac{T_d + iT_I - T_{\text{sensing}}}{T_{i,u}^{(s)}}. \quad (57)$$

Then the probability that the DBF fBS successfully obtains the channel is:

$$\begin{aligned} P_{\text{DBFsuc}} &= \sum_{i=i_0}^{\infty} \tilde{P}_i^{(c)} P_{\text{Suc},i}^{(c)} + \sum_{i=i_0}^{\infty} \sum_{u=1}^{N_W} \tilde{P}_{(i,u)}^{(s)} P_{\text{Suc},(i,u)}^{(s)} \\ &= \begin{cases} P_I Q_I^{i_0-1}(T_d + i_0 T_I - T_{\text{sensing}} + \frac{T_I Q_I}{1-Q_I})/T_{\text{avg}}, \\ \qquad\qquad\qquad\qquad\qquad\qquad \text{if } i_0 \geq 1 \\ (T_d - T_{\text{sensing}} + \frac{T_I P_I}{1-Q_I})/T_{\text{avg}}, \quad \text{if } i_0 = 0. \end{cases} \end{aligned} \quad (58)$$

Note that P_{DBFsuc} does not depend on T_{attempt} and T_{cellTx}. We can then obtain t_f from (48) using the P_{DBFsuc} computed in (58).

The analysis above provides an exact relationship between t_f and the parameters of both DBF and the non-cellular WLAN. In particular, it is shown in (48) that t_f depends on η and P_{DBFsuc}, where η is a DBF channel access parameter. P_{DBFsuc} as shown in (58) is a function of the non-cellular WLAN parameters, N_W, T_I, P_I, Q_I and T_{avg}, the latter three of which can be computed when the data rates and payload lengths of all the wDevices and the AP are known. While this analytical relationship helps us understand how t_f can be adjusted by varying DBF channel access parameter η, to directly apply it in practice, data rates and payload lengths of the AP and wDevices need to be obtained. As an alternative, we propose the following practical method to obtain P_{DBFsuc}.
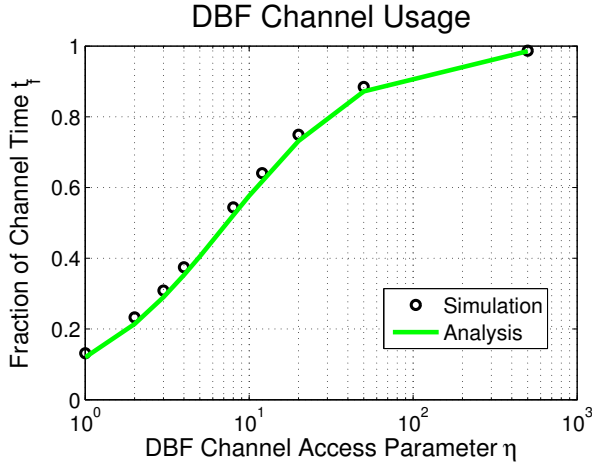
DBF Channel Usage

Fig. 8. DBF channel usage t_f from analysis and simulations. Markers are simulation results and curves are the numerical results of the analysis in this section (Sec. VI-A).

The fBS can directly estimate P_{DBFsuc} based on its recent channel access records,

$$P_{\text{DBFsuc}} = N_s / N_{\text{attempt}}, \tag{59}$$

where N_{attempt} is the total number of channel access attempts, out of which N_s turn out to be successful. This method requires no parameter knowledge of wDevices. Using the P_{DBFsuc} obtained in (59), the fBS can further obtain t_f via (48). This practical method will be used to obtain the traffic balancing simulation results reported in Section VII.

B. Validation of the Analysis

We carry out a simulation study to validate the analysis in Sec. VI-A. We consider a WLAN consisting of one AP and three wDevices, and a DBF consisting of one fBS and one sDevice. Recall that the DBF uses the unlicensed band for downlink traffic only, whereas the WLAN uses the unlicensed band in both uplink and downlink. The analytical and simulation results are obtained based on a fixed WiFi data rate 72Mbps and a packet payload length of 1500 bytes.

We fix T_{attempt} to 1ms and vary T_{cellTx} from 1ms to 500ms, hence η varies from 1 to 500. The impact of η on DBF channel usage t_f is shown in Fig. 8. The curve labeled "Analysis" is obtained from (48) using the P_{DBFsuc} computed in (58). Recall that all parameters in (58) can be computed as functions of the data rates and payloads of all WLAN devices and WLAN protocol parameters provided in the 802.11 standards. The curve labeled "Simulation" is obtained from the simulation data for t_f.

We observe from Fig. 8 that the simulation results match analytical results well. As predicted by (48), DBF channel time t_f is an increasing function of η. Additional simulations with different T_{attempt} values lead to similar results as shown in Fig. 8 and are not shown here. This demonstrates that η is the main DBF parameter that impacts DBF channel usage, which is consistent with our analytical results in (48).

t_{max} = 0.9	No. of Lic. subchannels K: 30
I_k = -100 dBm, $k = 1, 2, \ldots, K$	
IP Packet Size:	1500 Bytes
Transmit Power mBS: 40 dBm	fBS/WLAN AP: 15 dBm
Noise Power:	-95 dBm (over 20MHz BW)
Path Loss Models for Licensed and Unlicensed Bands	
mBS $\leftrightarrow$ mDevice PL = 15.3 + 37.6 $\log_{10}(R)$	
mBS or mDevice $\leftrightarrow$ fBS or sDevice PL = 15.3 + 37.6 $\log_{10}(R) + L_{ow}$, L_{ow} = 10dB	
fBS $\leftrightarrow$ associated sDevices WLAN AP $\leftrightarrow$ associated stations PL = 38.46 + 20 $\log_{10}(R)$ + 0.7R	
fBS or sDevice $\leftrightarrow$ fBS or sDevice in different cells, AP or station $\leftrightarrow$ AP or station in different WLANs, fBS or sDevice $\leftrightarrow$ WLAN AP or station PL = 15.3 + 37.6 $\log_{10}(R) + L_{ow}$, L_{ow} = 20dB	

VII. PERFORMANCE EVALUATION

In this section, we evaluate the proposed traffic balancing strategy in practical deployment scenarios. The simulation platform in [29] [30], a customized event-driven IEEE 802.11 network simulator built in C language, is extended to simulate the activities and interactions of macrocell, small cell and non-cellular WLANs in both licensed and unlicensed bands. The simulator models random packet arrivals at the IP layer, channel access schemes (for macrocell, small cell and WLAN) at the MAC layer, and includes interference computation and SINR-to-throughput mappings at the PHY layer. Table I summarizes the path loss models and parameters used in the simulations. The path loss models are based on a Small Cell Forum whitepaper [31], where path loss (PL) is in dB, distance R is in meters, and L_{ow} is the outer wall penetration loss.

LTE-Advanced [5] is adopted as the cellular air interface while 802.11n [32] with a frame aggregation level of 15K Bytes is used for the WiFi air interface. The bandwidth of WiFi is set 20 MHz. The approximate LTE rate function described in Section IV-G is used in the simulations.

We consider the following four use cases where a user or a group of users simultaneously use multiple sDevices and wDevices as shown in Fig. 2.

- Case 1 (Cellular WiFi Hotspot): Each small cell operates only in the unlicensed band using 802.11n air interface. The WiFi hotspot is used by both sDevices and wDevices.
- Case 2 (Separate Femto+WLAN): Each small cell (femtocell) operates only in licensed bands with the LTE air interface. In order to serve wDevices, the femtocell is deployed together with a WiFi AP. The femto BS and the WiFi AP are physically separate.
- Case 3 (IFW): Each small cell (IFW) [3] operates in licensed and unlicensed bands with LTE and WiFi air interfaces, respectively. The IFW is used by both sDevices and wDevices; there is no need to deploy additional WiFi APs. The simplest scheme ("IFW, Simple") uses equal power in all subchannels and fixed t_f (set to 0.8). We also consider the optimal traffic balancing strategy described in Section IV ("IFW, Optimal").
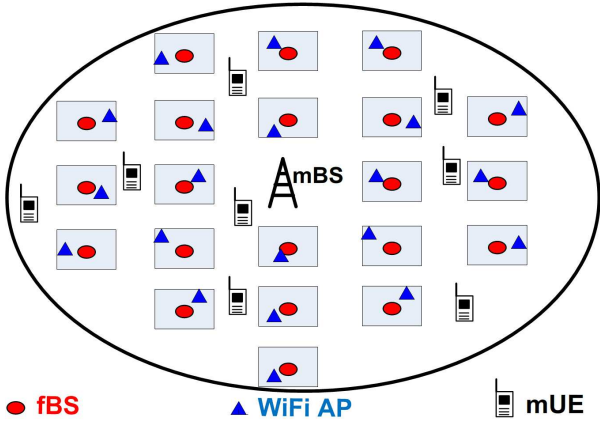
Fig. 9. The network topology used in simulations (sDevices and wDevices are not shown). The WiFi AP is shown for Cases 2 and 4 only; there is no WiFi AP in Case 1 or 3.

- Case 4 (DBF+WLAN): Each small cell (DBF) operates in both licensed and unlicensed bands with LTE air interface. In order to serve wDevices, the DBF is deployed together with a WiFi AP. The simplest scheme ("DBF+WLAN, Simple") uses equal power in all sub-channels and fixed t_f (set to 0.8). We also consider the optimal traffic balancing strategy described in Section IV ("DBF+WLAN, Optimal"). The DBF channel access scheme in the unlicensed band is described in Section III.

A. A simple scenario

We first consider a very simple scenario, in order to understand the intuitions behind our algorithms better. As aforementioned, the existing studies [2] mainly focus on power control; whereas this work focuses on both time-sharing control (in the unlicensed bands) and power control (in the licensed band). To understand the gain from time-sharing control alone, we assume there is only one fBS, one sDevice, one wDevice and no macrocell, which eliminates inter-cell interference in the licensed band. Recall that we do not consider fading, so the optimal power allocation scheme is the same as the "simple" scheme that assigns equal power to the subchannels. In addition, In Case 1, the short-range user only uses the unlicensed band; while in the other three cases, the user uses both licensed and unlicensed bands. To minimize the impact of the small cell frequency bandwidth imbalance between Case 1 and the other three cases, we assume that LTE licensed bandwidth is 1.4MHz which is the lowest allowed LTE bandwidth. Note that the unlicensed bandwidth is 20MHz. The sDevice and wDevice downlink traffic loads are 300Mbps (always full buffer) and 35Mbps (may not always be full buffer), respectively. Uplink traffic of each device is disabled to simplify the scenario.

Table (II) shows the simulation results, from which we have the following observations.

- The "Separate Femto+WLAN" case has much lower sum throughput and sum utility than the other cases, because the sDevice can only use the 1.4MHz licensed band,

whereas the sDevice in the other cases can share the 20MHz unlicensed band with the wDevice.
- DBF cases have higher sum throughput than the other cases, because of the higher efficiency of LTE than WiFi at the MAC layer. For 20MHz bandwidth, the simulator assumes that LTE and WiFi physical layer rates are 78Mbps and 72Mbps, respectively. But the maximum achievable MAC layer throughput are 75Mbps and 61Mbps, respectively. This is mainly because WiFi MAC protocol is distributed and contention-based, which incurs much channel access overhead (e.g., random backoff); whereas LTE MAC is centralized where the network schedules resources for each device.
- Compared with "DBF+WLAN, Simple" case, "DBF+WLAN, Optimal" case has lower sum throughput but higher sum utility. This is mainly due to the traffic balancing in the unlicensed band: $t_f = 0.8$ is used by "DBF+WLAN, Simple" case, whereas in the "DBF+WLAN, Optimal" case, the intuitions from Section IV-D suggest that our traffic balancing algorithm translates the total sDevice throughput (of licensed and unlicensed bands) into the unlicensed band channel time t'_f (=38Mbps/78Mbps=0.49), and tries to guarantee that t'_f is an *equal share of the combined channel time* $(t'_f + t^*_w)$ (t^*_w=33.7Mbps/72Mbps=0.47). The resulting optimal t^*_f is 0.42 in this case. The same observation can be made by comparing results between "IFW, Simple" and "IFW, Optimal" cases.
- In "WiFi hotspot" case, the throughput disparity between sDevice and wDevice is small, due to the natural long-term fairness of WiFi MAC protocol (sDevice throughput is slightly higher than wDevice due to higher sDevice traffic load), so the effective t_f is close to the optimal t^*_f (=0.45) for zero-Hz licensed bandwidth (see Fig. 5(a)). As a result, the sum utility (34.5) is very close to that of the "IFW, Optimal" case (34.6).

B. A realistic scenario

A suburban deployment scenario with a topology shown in Fig. 9 is considered. A mBS is placed at the center of the macrocell with radius 700m. Thirty (30) mDevices are randomly dropped in the macrocell with uniform distribution. Due to the uniformly distributed mDevice locations, some mDevices may be very close to fBSs. We assume that houses are located on 2D grid points with a center-to-center distance of 70m. Forty (40) houses are randomly selected; each selected house is given one sDevice and one wDevice, which are randomly placed within the fBS coverage area with a radius of 20m. In the use case of DBF, a WiFi AP is also placed in the selected house with a coverage radius of 20m. In this topology, the interference between houses is small, so each house is like an "island". Therefore, the algorithm developed in the previous section is applicable to this topology. Although the traffic-balancing algorithm does not consider the interference among houses, other parts of our simulator (e.g., SINR evaluation) do.

We consider the scenario where the aggregate uplink and downlink wDevice load is 35Mbps (50% of which is for

TABLE II
SIMULATIONS RESULTS FOR SCENARIO 1: NO MACROCELL (ONLY ONE fBS, ONE WiFi AP, ONE sDEVICE AND ONE wDEVICE), LTE LICENSED
BANDWIDTH 1.4MHz, wDEVICE LOAD 35MBPS

Use Cases	WiFi Hotspot	Separate Femto+WLAN	IFW Simple	IFW Optimal	DBF+WLAN Simple	DBF+WLAN Optimal
sDevice Throughput (Mbps)	32.8	5.5	51.7	30.7	66.9	38.0
wDevice Throughput (Mbps)	28.5	35.0	11.6	35.0	11.7	33.7
Sum device Throughput (Mbps)	61.3	40.5	63.3	65.7	78.6	71.7
User Utility	34.5	32.9	34.0	34.6	34.3	34.8

uplink), which is lower than the highest physical layer data rate 72Mbps for single-antenna 802.11n and lower than the highest achievable MAC layer throughput 61Mbps in our setup. Figures 10 and 11 show the throughput per device, utility per device, and utility per user. Note that each small cell user uses one sDevice and one wDevice; whereas each macro user uses one mDevice. We have the following observations from the figures. First, the small cell optimal traffic-balancing algorithm significantly improves mDevice performance, while it does not significantly affect the performance of sDevice or wDevice. This can be verified by comparing scenario "IFW, Simple" with "IFW, Optimal," and "DBF+WLAN, Simple" with "DBF+WLAN, Optimal." The is mainly due to the licensed band power control included in the algorithm which reduces the interference from small cells to the macrocell. Second, using two bands simultaneously as in the IFW and DBF improves the average utility and throughput of *all devices*. The proposed traffic-balancing strategy shown in "IFW, Optimal" and "DBF+WLAN, Optimal" obtain higher average utilities than the other cases, including "IFW, Simple" and "DBF+WLAN, Simple." Third, there is very little utility or throughput difference between the IFW and DBF cases. Forth, the "WiFi Hotspot" scenario has better good macro user utility, which is mainly due to no interference to mDevice; in contrast, the fBSs in "DBF+WLAN, Optimal" and "IFW, Optimal" cases can only reduce, but not eliminate, interference to mDevices. While the proposed traffic-balancing algorithm does not obtain the highest average throughput, this is not surprising, since it is designed to achieve performance fairness through the utility function. Note that in all cases discussed, the total bandwidth is 30 MHz (licensed 10 MHz, unlicensed 20 MHz); however, the way this bandwidth is shared among classes of devices is different in each case.

VIII. DISCUSSIONS AND CONCLUSION

Small cells have been considered as effective means to boost the wireless capacity. In this paper, we have described the dual-band femtocell (DBF) that simultaneously uses the LTE air interface in licensed and unlicensed bands based on the LTE carrier aggregation feature. We have proposed a channel access scheme for DBFs to access the unlicensed band. Furthermore, we have described a traffic balancing algorithm for small cells, including the DBF and the Integrated Femto-WiFi (IFW)
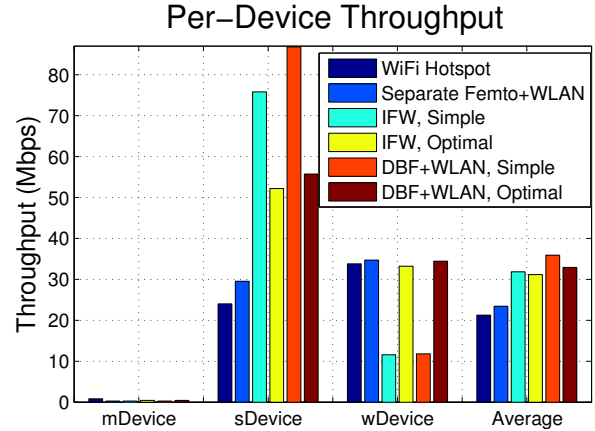

Fig. 10. Per-device throughput when the aggregate wDevice load is 35Mbps (the highest WiFi physical layer rate is 72Mbps). The "Average" metric is averaged over all mDevices, sDevices and wDevices.

proposed by the Small Cell Forum, to use both licensed and unlicensed bands in an optimized fashion thereby improving the overall user utility/satisfaction from macrocell, small cell and non-cellular WiFi-only devices. The algorithm searches for the optimal power allocation in the licensed band, and the optimal channel time usage in the unlicensed band. We have also proposed practical algorithms to tune the unlicensed-band channel time usages for IFWs and DBFs, which uses the WiFi and LTE air interfaces in the unlicensed band, respectively. Our results illustrate that, in terms of average user utility, both IFW and DBF outperform current WiFi hotspot and femtocell approaches and thus are attractive technologies for emerging small cell applications. While IFW and DBF have comparable performance, we have the following observations from an implementation perspective.

- **IFW:** The IFW has separate cellular and WiFi radio interfaces in licensed and unlicensed bands. Hence, it is backward compatible with existing cellular and WLAN devices. However, special effort is required for a single application flow to simultaneously use two radio interfaces [3].
- **DBF:** The DBF is actively under 3GPP LTE standardization [6], where the unlicensed band is a secondary carrier in carrier aggregation. Therefore, the DBF has a
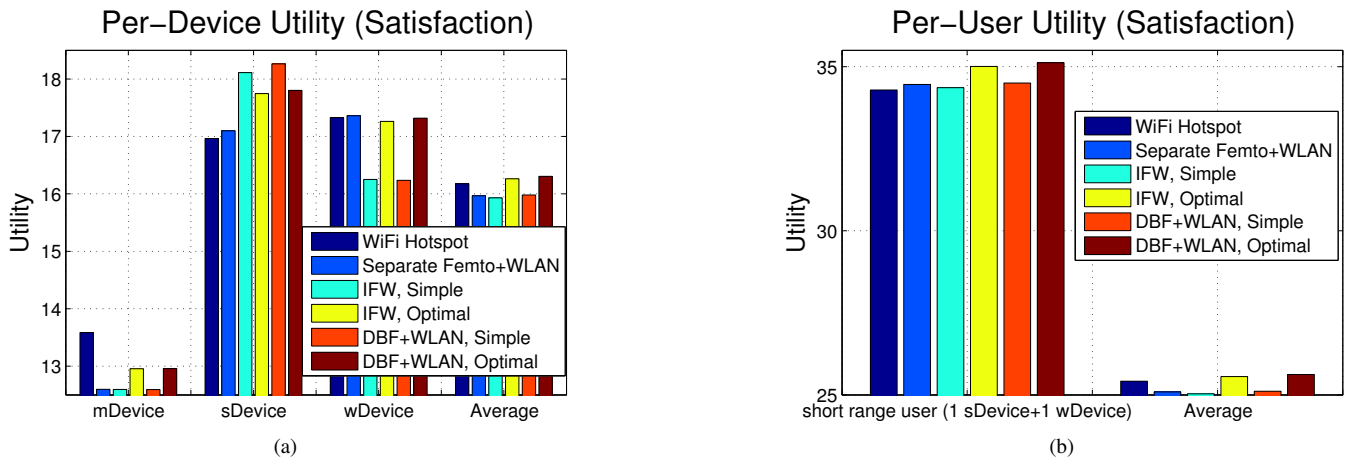
Fig. 11. Per-device and per-user utilities when the aggregate wDevice load is 35Mbps. In Fig. 11(a), the "Average" metric is averaged over all mDevices, sDevices and wDevices; In Fig. 11(b), the "Average" metric is averaged over 30 macro users and 40 small cell users.

single radio interface. The DBF BS informs its devices, via licensed-band control channel, about when and which subchannel to receive their data in both licensed and unlicensed bands. The DBF is backward compatible with existing LTE devices. However, the DBF cannot serve WiFi-only devices. Therefore, it should be deployed or integrated with WiFi APs to serve WiFi-only devices.

REFERENCES

[1] V. Chandrasekhar, J. Andrews, and A. Gatherer, "Femtocell networks: a survey," *IEEE Comm. Mag.*, pp. 59–67, Sep. 2008.
[2] S. Rangan, "Femto-macro cellular interference control with subband scheduling and interference cancelation," *arXiv*, [Online] http://arxiv.org/abs/1007.0507, 2010.
[3] Small Cell Forum, "Integrated Femto-WiFi (IFW) networks," Whitepaper at smallcellforum.org, Feb. 2012.
[4] F. Liu, E. Bala, E. Erkip, and R. Yang, "A framework for femtocells to access both licensed and unlicensed bands," in *Proc. of the third International Workshop on Indoor and Outdoor Femto Cells (IOFC)*, Princeton, NJ, USA, May 13, 2011.
[5] 3GPP TS 36.300 v10.2.0, "E-UTRA and E-UTRAN; Overall description; Stage 2 (Release 10)," 2011.
[6] Ericsson, Qualcomm, Huawei, Alcatel-Lucent, "Study on licensed-assisted access using LTE," *RP-141664, 3GPP TSG RAN Meeting 65,*, Edinburgh, Scotland, 9-12 Sept. 2014.
[7] F. Liu, E. Erkip, M. Beluri, R. Yang, and E. Bala, "Dual-band femtocell traffic balancing over licensed and unlicensed bands," in *Proc. of IEEE ICC*, Ottawa, ON, Canada, 10-15 June 2012.
[8] M. Rahman, A. Behravant, H. Koorapaty, J. Sachs, and K. Balachandran, "License-exempt LTE systems for secondary spectrum usage: Scenarios and first assessment," in *Proc. of IEEE Symposium on New Frontiers in Dynamic Spectrum Access Networks (DySPAN)*, May 2011.
[9] L. Sun, "The unlicensed spectrum usage for future IMT technologies," in *Proc. of The 6th International Workshop - Vision and Technology Trends for 5G*, Seoul, Korea, Sept. 04, 2013.
[10] M. Bennis, M. Simsek, A. Czylwik, W. Saad, S. Valentin, and M. Debbah, "When cellular meets WiFi in wireless small cell networks," *IEEE communications magazine*, vol. 51, Jun. 2013.
[11] A. Elsherif, W.-P. Chen, A. Ito, and Z. Ding, "Adaptive small cell access of licensed and unlicensed bands," [Online] http://www.fujitsu.com/downloads/SVC/fla/research/Adaptive-Small-Cell-Access-of-Licensed-and-Unlicensed-Bands.pdf , 2013.
[12] N. Ksairi, P. Bianchi, and P. Ciblat, "Nearly optimal resource allocation for downlink ofdma in 2-D cellular networks," *IEEE Trans. On Wireless Comm.*, vol. 10, pp. 2101–2115, July 2011.
[13] IEEE Std 802.11-2007 (Revision of Std 802.11-1999), "Part II: Wireless LAN MAC and PHY Specifications," 2007.
[14] J. Mo and J.Walrand, "Fair end-to-end window-based congestion control," *IEEE Trans. Netw.*, pp. 556–567, Oct. 2000.
[15] D. Bertsekas and R. Gallager, *Data Networks*. Prentice Hall, 1992.
[16] G. Bianchi, "Performance analysis of the IEEE 802.11 distributed coordination function," *IEEE Journal on Selected Areas in Communications*, vol. 18, pp. 535–547, Mar. 2000.
[17] C. H. Foh and J. W. Tantra, "comments on IEEE 802.11 Saturation Throughput Analysis with Freezing of Backoff Counters," *IEEE Communications Letters*, vol. 9, pp. 130–132, Feb. 2005.
[18] Y. Lee, D. H. Han, and C. G. Park, "IEEE 802.11 saturation throughput analysis with freezing of backoff counters," in *Proc. of ICCOM'05*, Stevens Point, Wisconsin, USA, 2005.
[19] S. P. Boyd and L. Vandenberghe, *Convex Optimization*. Cambridge Univ. Press, 2004.
[20] K. Son, B. C. Jung, S. Chong, and D. K. Sung, "Opportunistic underlay transmission in multi-carrier cognitive radio systems," in *Proc. of WCNC 2009*.
[21] N. Papandreou and T. Antonakopoulos, "Bit and power allocation in constrained multicarrier systems: The single-user case," *EURASIP JNL on Advances in Signal Processing*, Article ID 643081, Oct. 2008.
[22] P. Mogensen, W. Na, I. Kovacs, F. Frederiksen, A. Pokhariyal, K. Pedersen, T. Kolding, K. Hugl, and M. Kuusela, "LTE capacity compared to the shannon bound," in *Proc. of Vehicular Technology Conference (VTC2007-Spring)*, April 2007.
[23] 3GPP TR 36.921 v10.0.0, "E-UTRA; FDD home eNode B (HeNB) radio frequency (RF) requirements analysis," 2011.
[24] A. Adhikary, V. Ntranos, and G. Caire, "Cognitive femtocells: Breaking the spatial reuse barrier of cellular systems," in *Proc. of Information Theory and Applications Workshop (ITA)*, Feb. 2011.
[25] W. C. Suski, M. A. Temple, M. J. Mendenhall, and R. F. Mills, "Radio frequency fingerprinting commercial communication devices to enhance electronic security," *Int'l Journal of Electronic Security and Digital Forensics*, pp. 301–322, Oct 2008.
[26] H. Kim, S. Yun, I. Kang, and S. Bahk, "Resolving 802.11 performance anomalies through QoS differentiation," *IEEE Communications Letters*, pp. 655–657, July 2005.
[27] W. H. Press, B. P. Flannery, S. A. Teukolsky, and W. T. Vetterling, *Numerical recipes in Fortran: the art of scientific computing, 2nd ed.* Cambridge University Press, 1992.
[28] M. Heusse, F. Rousseau, G. Berger-Sabbatel, and A. Duda, "Performance anomaly of 802.11b," in *Proc. of INFOCOM*, 2003.
[29] P. Liu, Z. Tao, Z. Lin, E. Erkip, and S. S. Panwar, "Cooperative wireless communications: a cross layer approach," *IEEE Wireless Communications*, vol. 13, pp. 84–92, Aug. 2006.
[30] P. Liu, Z. Tao, S. Narayanan, T. Korakis, and S. S. Panwar, "CoopMAC: a cooperative MAC for wireless LANs," *IEEE Journal on Selected Areas in Communications*, vol. 25, pp. 340–354, Feb. 2007.
[31] Small Cell Forum, "Interference management in OFDMA femtocells," Whitepaper at smallcellforum.org, Mar. 2010.
[32] IEEE Std 802.11n-2009, "Part 11: Wireless LAN MAC and PHY Specifications," 2009.
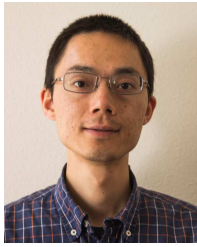
Feilu Liu Feilu Liu received the B.E. degree in electronic engineering from Southeast University, Nanjing, China, and the M.S. and Ph.D. degrees in electrical engineering from Polytechnic school of engineering, New York University. He has been with Qualcomm Technologies, CA as a systems engineer since 2012. His previous work experience includes software engineer at Alcatel-Lucent, China and intern at InterDigital, NY. He has been working on the systems design for LTE MAC/RLC/PDCP/RRC layer implementations. He is interested in wireless networking protocol and algorithm design.

Mihaela Beluri Mihaela Beluri (M'90) received the M.S. degree in electrical engineering from the Polytechnic University of Bucharest, Romania. She is currently a Principal Engineer with InterDigital Communications, Melville, NY, working on millimeter wave technologies. Her recent experience includes dynamic spectrum management and shared spectrum technologies, algorithm design, modeling and simulations for WCDMA, HSPA and LTE systems. She has authored or coauthored IEEE conference publications and holds several patents.

Erdem Bala Erdem Bala got his BSc and MSc degrees from Bogazici University, Istanbul, Turkey and his PhD degree from the University of Delaware, DE, all in electrical engineering. He has been with InterDigital, NY as a research engineer since 2007. His previous work experience includes positions as R&D engineer at Nortel Networks and intern at Mitsubishi Research Labs. At InterDigital, he has worked on the standardization of 3GPP LTE and LTE-Advanced, advanced relaying schemes, coexistence in unlicensed spectrum, and waveform design. Currently, he is involved in the design of 5G air interface for future wireless communication systems.

Elza Erkip Elza Erkip (S'93-M'96-SM'05-F'11) received the B.S. degree in electrical and electronics engineering from Middle East Technical University, Ankara, Turkey, and the M.S. and Ph.D. degrees in electrical engineering from Stanford University, Stanford, CA, USA. Currently, she is a Professor of electrical and computer engineering with New York University Polytechnic School of Engineering, Brooklyn, NY, USA. Her research interests are in information theory, communication theory, and wireless communications.

Dr. Erkip is a member of the Science Academy Society of Turkey and is among the Thomson Reuters 2014 Edition of Highly Cited Researchers. She received the NSF CAREER award in 2001, the IEEE Communications Society Stephen O. Rice Paper Prize in 2004, the IEEE ICC Communication Theory Symposium Best Paper Award in 2007, and the IEEE Communications Society Award for Advances in Communication in 2013. She co-authored a paper that received the IEEE International Symposium on Information Theory Student Paper Award in 2007. Currently, she is a Member of the Board of Governors of the IEEE Information Theory Society and a Guest Editor of the IEEE JOURNAL ON SELECTED AREAS IN COMMUNICATIONS. Dr. Erkip was a Distinguished Lecturer of the IEEE Information Theory Society from 2013 to 2014, an Associate Editor of the IEEE TRANSACTIONS ON INFORMATION THEORY from 2009 to 2011, an Associate Editor of the IEEE TRANSACTIONS ON COMMUNICATIONS from 2006 to 2008, a Publications Editor of the IEEE TRANSACTIONS ON INFORMATION THEORY from 2006 to 2008 and a Guest Editor of the IEEE SIGNAL PROCESSING MAGAZINE in 2007. She was a General Chair for the IEEE International Symposium of Information Theory in 2013, a Technical Program Chair for the International Symposium on Modeling and Optimization in Mobile, Ad Hoc, and Wireless Networks (WiOpt) in 2011, a Technical Program Chair for the IEEE GLOBECOM Communication Theory Symposium in 2009, the Publications Chair for the IEEE Information Theory Workshop, Taormina, in 2009, the Technical Area Chair for the MIMO Communications and Signal Processing track of Asilomar Conference on Signals, Systems, and Computers in 2007, and a Technical Program Chair for the IEEE Communication Theory Workshop in 2006.

Rui Yang Rui Yang received the M.S. and Ph.D. degrees in electrical engineering from the University of Maryland, College Park, in 1987 and 1992, respectively. He has 15 years of experience in the research and development of wireless communication systems. Since he joined InterDigital Communications in 2000, he has led several product development and research projects. He is currently a Principle Engineer at InterDigital Labs, leading a project on baseband and RF waveforms for future wireless communication systems. His interests include digital signal processing and air interface design. He has received more than 15 patent awards in those areas.